European Journal of Pharmaceutics and Biopharmaceutics 158 (2021) 185–197

Contents lists available at ScienceDirect

European Journal of Pharmaceutics and Biopharmaceutics

journal homepage: www.elsevier.com/locate/ejpb

Two-step *in vitro-in vivo* correlations: Deconvolution and convolution methods, which one gives the best predictability? Comparison with one-step approach

Bárbara Sánchez-Dengra, Ignacio González-García, Marta González-Álvarez, Isabel González-Álvarez *, Marival Bermejo

Engineering: Pharmacokinetics and Pharmaceutical Technology Area, Miguel Hernandez University, Spain

ARTICLE INFO

Keywords:
IVIVC
Bioequivalence
BCS
Predictive *in vivo*-dissolution
One-step
Two-step

ABSTRACT

Finding predictive dissolution tests and valid IVIVCs are essential activities in generic industry, as they can be used as substitutes of human bioequivalence studies. IVIVCs can be developed by two different strategies: a one-step approach or a two-step approach.

The objectives of this work were to compare different deconvolution and convolution methods used in the development of two-step level A IVIVCs and to study if the relationship between the *in vitro* dissolution rate and the *in vivo* dissolution rate should guide the decision between using a two-step approach or a one-step approach during the development of a new IVIVC.

When the *in vitro* and the *in vivo* dissolution rates had a linear relationship, valid and biopredictive two-step IVIVCs were obtained, although there was not a combination of deconvolution and convolution methods that could be named as the best one, as long as all the prediction errors for any combination were within the limits.

It was not possible to obtain a valid two-step IVIVC when the relationship between dissolution rates was non-linear, but the one-step approach was able to overcome this fact and it gave valid IVIVCs regardless of whether the relationship between dissolution rates was linear or non-linear.

1. Introduction

Finding predictive dissolution tests is an essential activity in generic industry, as, depending of the drugs, they can be used as substitutes of human bioequivalence studies.

Biopharmaceutics classification system (BCS) divides drugs in four groups or classes depending on their permeability and on their solubility: Class I) high permeability-high solubility drugs, class II) high permeability-low solubility drugs, class III) low permeability-high solubility drugs and class IV) low solubility-low permeability drugs. It is assumed that a drug has a high solubility if its highest dose is completely dissolved in 250 mL of physiological pH aqueous media and it has a high permeability if the 90% or more of the administered dose is absorbed [1–3].

This classification is used by competent agencies, as the Food and Drug Administration (FDA) or the European Medicines Agency (EMA), to define which formulations can demonstrate bioequivalence just with dissolution tests (biowaiver) and which ones must go to human bioequivalence studies. Biowaivers are allowed for class I and class III drugs as, if they are dissolved quickly, their limiting step to drug absorption is

Abbreviations: BCS, Biopharmaceutics classification system; FDA, Food and Drug Administration; EMA, European Medicines Agency; IVIVC, *In vitro/in vivo* correlation; Cp and C_t, Plasma concentration; f_a, Absorbed fractions; f_{diss}, Dissolved fractions; Q_{diss}, Quantity dissolved; Q_c, Quantity in central compartment; A_t, Absorbed concentration; E_t, Eliminated concentration; k_{el}, Elimination rate; k_a, Absorption rate; k_d, Dissolution rate; F_{max}, Maximum fraction dissolved; F, Bioavailability; D, Dose; AUC, Area under the curve; Cmax, Maximum concentration; V_d, Distribution volume; IV, Intravenous; EV, Extravascular; IRF, Inverse release function; PE%, Prediction error percentage; Exp, Experimental; Pred, Predicted; sc, Scaling factor; WN, Wagner-Nelson; PA, Point-area; CF, Curve fitting; NL, Without Levy plot; L, Linear; P, Polynomial; BWN, Back Wagner-Nelson; S, Superposition; G(t), Antitransform of the transfer function; r(t), response function; w(t-n), weighting function or unit impulse response function; i(t), input function.

* Corresponding author at: Edificio Muhammad Al-Shafra, Facultad de Farmacia, UMH, Carretera Alicante Valencia km 87, 03550 San Juan de Alicante, Alicante, Spain.

E-mail address: isabel.gonzalez@umh.es (I. González-Álvarez).

https://doi.org/10.1016/j.ejpb.2020.11.009
Received 1 September 2020; Received in revised form 9 November 2020; Accepted 19 November 2020
Available online 26 November 2020
0939-6411/© 2020 Elsevier B.V. All rights reserved.

gastric emptying. Conditions to be allowed to use predictive dissolution tests to demonstrate bioequivalence are the following ones:

- Formulations with class I drugs must have a fast dissolution speed, that is, the 85% of the drug must be dissolved in 30 min or less and this formulations must have the same qualitative and quantitative composition of the excipients that could affect bioavailability [2,3].
- Formulations of class III drugs must prove that they have a very fast dissolution (85% or more in 15 min or less) and the same qualitative and quantitative composition of excipients [2,3].

A special case is the formulation with class II drugs. In this case, a biowavier cannot be asked directly, but if a predictive dissolution test is found and it can simulate the *in vivo* dissolution process, the limiting step of drug absorption in this group, an *in vitro/in vivo* correlation could be established and it could be used as a substitute of human bioequivalence studies [4,5].

In vitro/in vivo correlations (IVIVCs) are mathematical models that can relate an *in vitro* characteristic of a drug with a characteristic of its *in vivo* behavior [6–8].

Their final aim is to predict plasma profiles of human people from the results of a dissolution test and, for reaching that goal, IVIVCs can be developed by following two different strategies: a one-step approach or a two-step approach [5].

The one-step approach allows predicted plasma profiles to be obtained directly from a combination of *in vitro* data and experimental *in vivo* plasma concentrations by mathematical modeling with differential equations. By its side, in the two-step approach, experimental plasma profiles must be, firstly, transformed to fractions absorbed by deconvolution, and the IVIVC is obtained by relating *in vitro* fractions dissolved with *in vivo* fractions absorbed; then, for being returned to plasma concentrations, predicted fractions absorbed are reconverted by convolution.

There is controversy about which approach is the best for constructing an IVIVC. The FDA recommends the use of the two-step approach [4], despite the limitations of the deconvolution methods that several authors have remarked in their publications [9,10]. The EMA, by its part, defends that deconvolution methods should be just used as exploratory tools and the one-step approach should be the methodology selected for developing IVIVCs [11], as convolution does not need, for instance, data collected at the same times and can predict plasma levels directly using individual data. Nevertheless, these methods assume linearity of the system and invariance in time.

There are lots of software to develop IVIVCs as: NONMEM® [12–14], SAS® [15], Sigma-Plot® [16], Excel® [17], PC_IVIVC® [18] and Phoenix WinNonlin [19–21].

The objectives of this work were: 1) to compare different deconvolution and convolution methods used in the development of two-step level A IVIVCs by analyzing their influence in their predictability and 2) to study if the relationship between the *in vitro* dissolution rate and the *in vivo* dissolution rate should guide the decision between using a two-step approach or a one-step approach during the development of a new IVIVC.

2. Experimental section

For carrying out this work, three batches of data were simulated with Nonmem®: one batch from an *in vitro* dissolution test and two batches from human bioequivalence studies, in the first one, it was assume that the *in vivo* dissolution rate had a linear relationship with the *in vitro* dissolution rate and, in the second one, it was assume that this relationship was non-linear and it followed a Hill equation. Two-step IVIVCs were obtained with Microsoft Excel® and one-step IVIVCs were developed with Berkeley-Madonna®.

1. Two-step IVIVCs

a. Deconvolution methods

Simulated *in vivo* plasma profiles for three no bioequivalent formulations (Fig. 1) were adjusted to a one-compartment disposition model and three different deconvolution methods were used for transforming plasma concentrations (Cp) to fractions absorbed (f_a): Wagner-Nelson, point-area and curve fitting.

2.1. Wagner-Nelson method

Wagner-Nelson deconvolution method is a mass balance based mathematical procedure with which absorption profiles can be calculated for those drugs that follow a one-compartment behaviour.

Wagner-Nelson method assumes that at time equal to infinite the total amount of absorbed drug is equal to the total amount of eliminated drug. At any other time, different to infinite, the absorbed concentration (A_t) will be equal to the addition of the plasma concentration at that time (C_t) and the eliminated concentration until that moment (E_t) [22].

Taking the foregoing condition into account, fractions absorbed (f_a) at each time can be calculated using the following equation (Eq. (1)), in which k_{el} is the elimination rate and AUC represents the area under the curve between 0 and different times or infinite [23].

$$f_a = \frac{A_t}{A_\infty} = \frac{C_t + E_t}{E_\infty} = \frac{C_t + k_{el}\cdot AUC_0^t}{k_{el}\cdot AUC_0^\infty} \tag{1}$$

2.2. Point-area method

The point-area method is a model-independent procedure that combines data from intravenous (IV) profiles and extravascular (EV) profiles for approximating the values of the fractions absorbed and the absorption constant without adjusting the behavior of the studied drug to a concrete pharmacokinetic model. This procedure can be used when the time intervals are always the same. The main equation that must be known for applying this method is the antitransform of the transfer function (G(t)). Equation (2) shows how the antitransform of the transfer function can be calculated at any time (t = n) [24].

$$G(t_n) = \frac{\left[C_{P_{EV}}(t_n) - \sum_{i=2}^{n} AUC_{IV}^{t_{i-1}\rightarrow t_i}\cdot G(t_{n-i+1})\right]}{AUC_{IV}^{0\rightarrow 1}} \tag{2}$$

In zero-order absorption processes and in first-order absorption processes, the antitransform of the transfer function is equal to the product of bioavailability (F) by the differential of the fractions absorbed versus time (Eq. (3)) [24].

$$G(t_n) = F\cdot\frac{dfa(t)}{dt} \approx F\cdot\frac{\Delta fa(t)}{\Delta t} \tag{3}$$

2.3. Curve fitting method

In the curve fitting method, a method model-dependent, the parameters that characterize the pharmacokinetic behavior of the drug under study are calculated through the simultaneous adjustment of plasma concentration profiles after an intravenous administration and an extravascular administration. In case of a one-compartment drug the equations for adjusting the profiles are the following ones (Eqs. (4) and (5)) [23].

$$IV\rightarrow C_{IV} = \frac{D_{IV}}{V_d}\cdot e^{-k_{el}\cdot t} \tag{4}$$

$$EV\rightarrow C_{EV} = F\cdot\frac{D_{EV}}{V_d}\cdot\frac{k_a}{k_a - k_{el}}\cdot\left(e^{-k_{el}\cdot t} - e^{-k_a\cdot t}\right) \tag{5}$$

Once the absorption constant is obtained, by minimizing the sum of residual squares of both adjustments, the fractions absorbed after the extravasal administration are calculated from it.

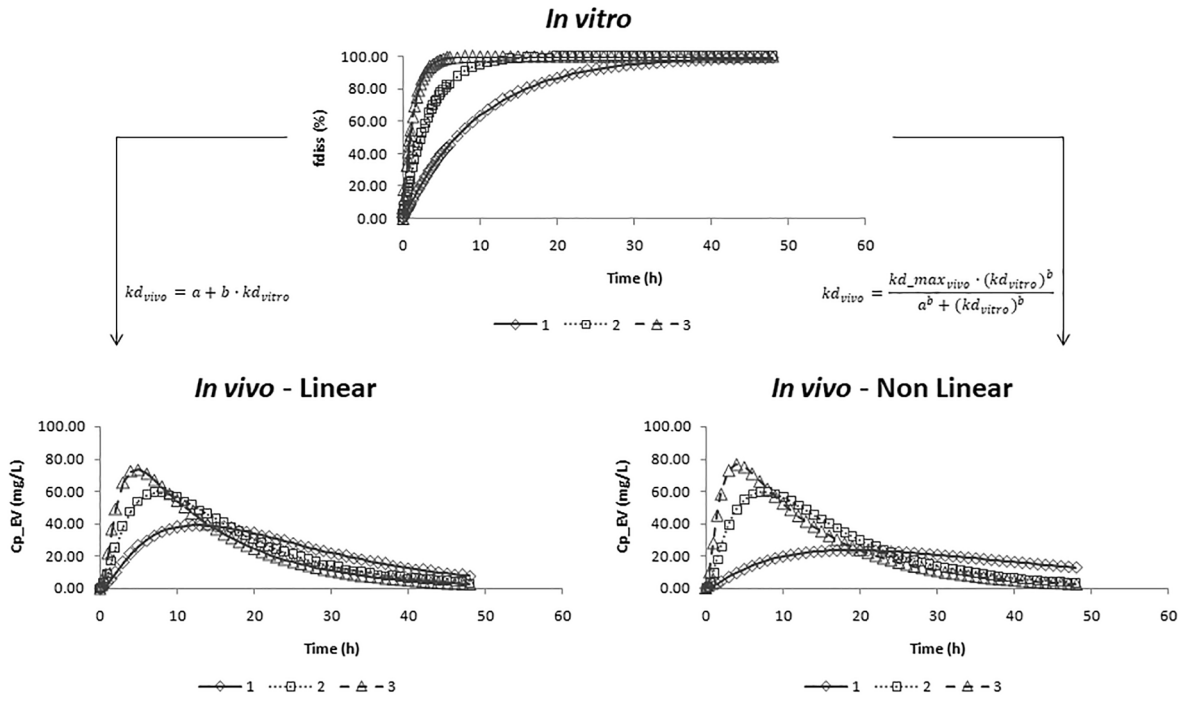

Fig. 1. Simulated *in vitro* dissolution and *in vivo* plasma profiles for three non-bioequivalent formulations (1, 2 and 3).

b. **Time scaling**

Once dissolution profiles have been obtained and experimental plasma profiles have been transformed into fractions absorbed by deconvolution, a level A IVIVC can be obtained by relating the fractions absorbed and the fractions dissolved at the same times.

However, this combination can be made directly just in case that both processes dissolution and absorption happen at the same speed and, thus, profiles are superimposable. This fact is not common and, normally, *in vitro* dissolution is faster than *in vivo*. If this happens, it is necessary a time scaling phase to make both processes overlapping.

In this study, the necessity of a time scaling phase was also studied by the construction of a Levy Plot and obtaining an inverse release function (IRF) as done previously in the literature [20,25–27].

c. **Convolution methods**

When the different two-step IVIVCs were obtained, predicted fractions absorbed were convoluted to predicted plasma profiles by two different methods: the back Wagner-Nelson method and the superposition method.

2.4. Back Wagner-Nelson method

This method is the equivalent of the Wagner-Nelson deconvolution method and it can be used, as the other one, when the drug follows a one-compartment disposition behaviour.

The following equation (Eq. (6)) can be used for obtaining the predicted plasma profiles by this method [28].

$$C_p(t-1) = \frac{\frac{2\times\Delta f_a\times D}{V_d} + C_p(t)\times(2 - k_{el}\times\Delta t)}{(2 + k_{el}\times\Delta t)} \quad (6)$$

2.5. Superposition method

This other convolution method is an approach, proposed by Langenbucher, which, as its name says, is based in the superposition principle [29]. This principle assumes: (1) dose proportionality and (2) time invariance; this is that:

(1) If an input (i(t)) gives rise to a response (r(t)), a multiplication or a fraction of that input (m*i(t)) will be equal to a multiplication or fraction of the response (m*r(t)).
(2) If an input is given to a time n other than zero, the response will be the same but displaced n.

The following equation (Eq. (7)) shows the convolution integral in which this principle is based.

$$r(t) = \int_0^t i(n)\times w(t-n)dn \quad (7)$$

In which,

- i(n) represents the input function into the system, i.e the fractional absorption rate,
- w(t-n) is the so-called weighting function or unit impulse response function and would correspond to the normalized disposition function (i.e the plasma profile after intravenous administration of a Dose = 1), and
- r(t) represents the response of the system to the oral administration.

That is the plasma profile after the oral administration (r(t), is the sum (integral operation) of a series of infinitesimal impulses (i(n)) multiplied by the disposition function (w(t-n). For a detailed derivation of the equation see [29].

2. **One-step IVIVCs**

One-step IVIVCs were developed with the software Berkeley-Madonna® and the libraries are shown in the supplementary material (S1).

3. **Internal validation**

The predictability of the obtained IVIVCs was evaluated by internal validation calculating the prediction error percentage (PE%) for the predicted AUC and the predicted Cmax (Eq. (8)).

$$PE\% = \frac{\text{Experimental parameter} - \text{Predicted parameter}}{\text{Experimental parameter}} \cdot 100 \quad (8)$$

FDA and EMA consider that an IVIVC is valid and, therefore, bio-predictive when it meets two conditions: the mean prediction error for each parameter is lower than 10% and the prediction error for each formulation and each parameter is below 15% [23].

3. Results

3.1. Simulated data

Fig. 1 shows the *in vitro* dissolution and *in vivo* plasma profiles simulated with NONMEM® for carrying out this study. All three formulations (1, 2 and 3) were simulated as non-bioequivalent *in vivo* and non-similar *in vitro*.

3.2. Deconvolution methods

Absorption profiles for the three formulations (1, 2 and 3) are shown in Fig. 2. Fig. 2 shows the f_a obtained by Wagner-Nelson method, point-area method and curve fitting method, for the case in which the *in vivo* dissolution rates have a linear relationship with the *in vitro* dissolution rate and, the case in which it is assumed that this relationship is non-linear.

3.3. Time scaling

For knowing if time scaling was necessary, both, *in vitro* dissolution profiles and *in vivo* fractions absorbed were represented in the same graph. Fig. 3 shows these representations for the absorption profiles obtained by the different deconvolution methods.

It can be seen that profiles were not perfectly overlapping and, because of that, a Levy Plot was constructed for each deconvolution approach and type of data (Fig. 4).

When data were simulated assuming a non-linear relationship between the *in vitro* dissolution rate and *in vivo* dissolution rate, the tendency of formulation one is completely different to the other two, at least when the Wagner-Nelson and Point Area deconvolution methods are used. Therefore, those Levy Plot were discarded and four different inverse release functions (IRFs) were obtained (Eq. (9)–(12)), with

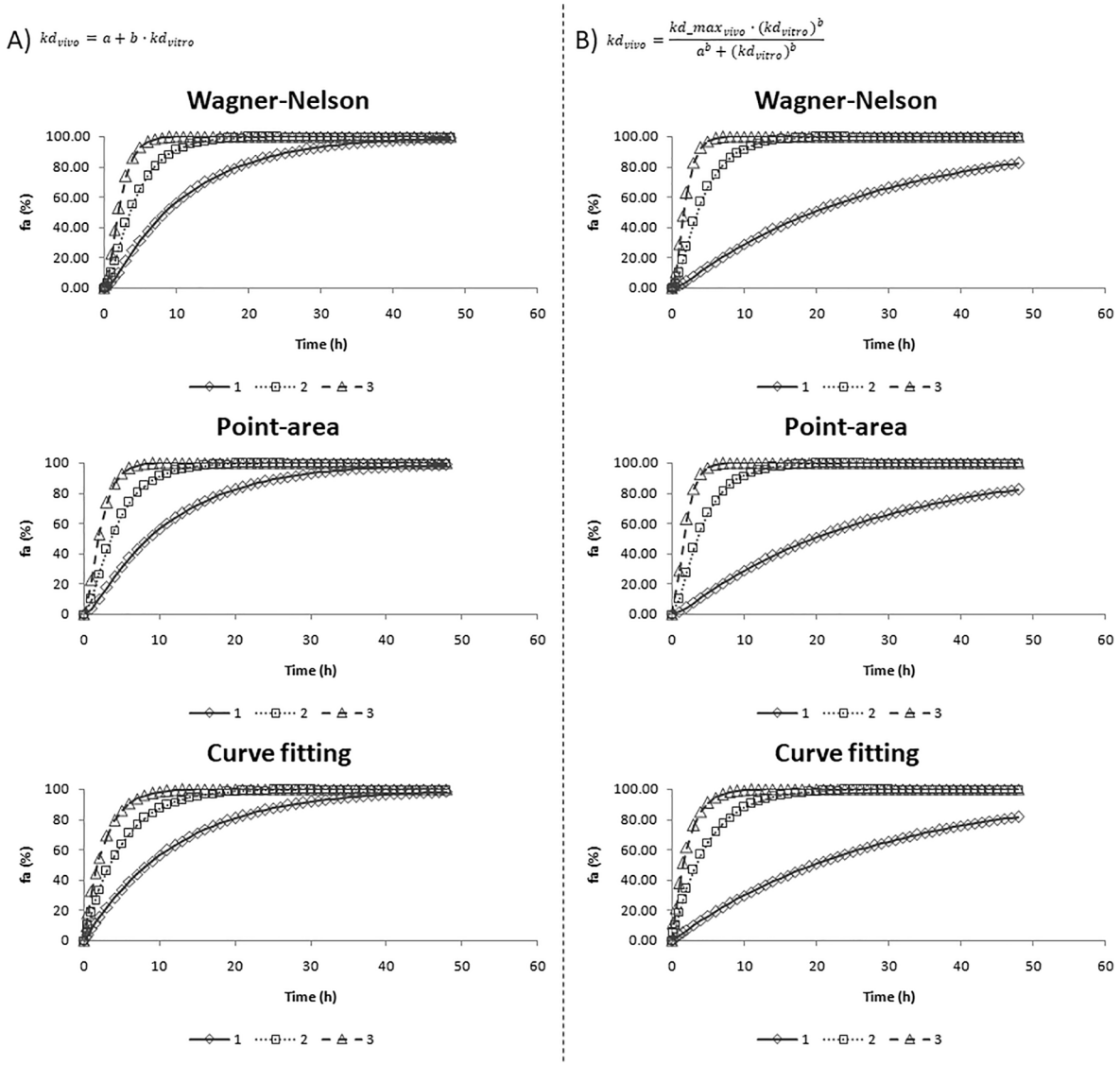

Fig. 2. Absorption profiles obtained by the three different deconvolution methods (Wagner-Nelson, Point-area and Curve fitting) for the three formulations (1, 2 and 3). A) Absorption profiles from the *in vivo* data simulated assuming a linear relationship between the *in vitro* dissolution rate and the *in vivo* dissolution rate. B) Absorption profiles from the *in vivo* data simulated assuming a non-linear relationship between the *in vitro* dissolution rate and the *in vivo* dissolution rate.

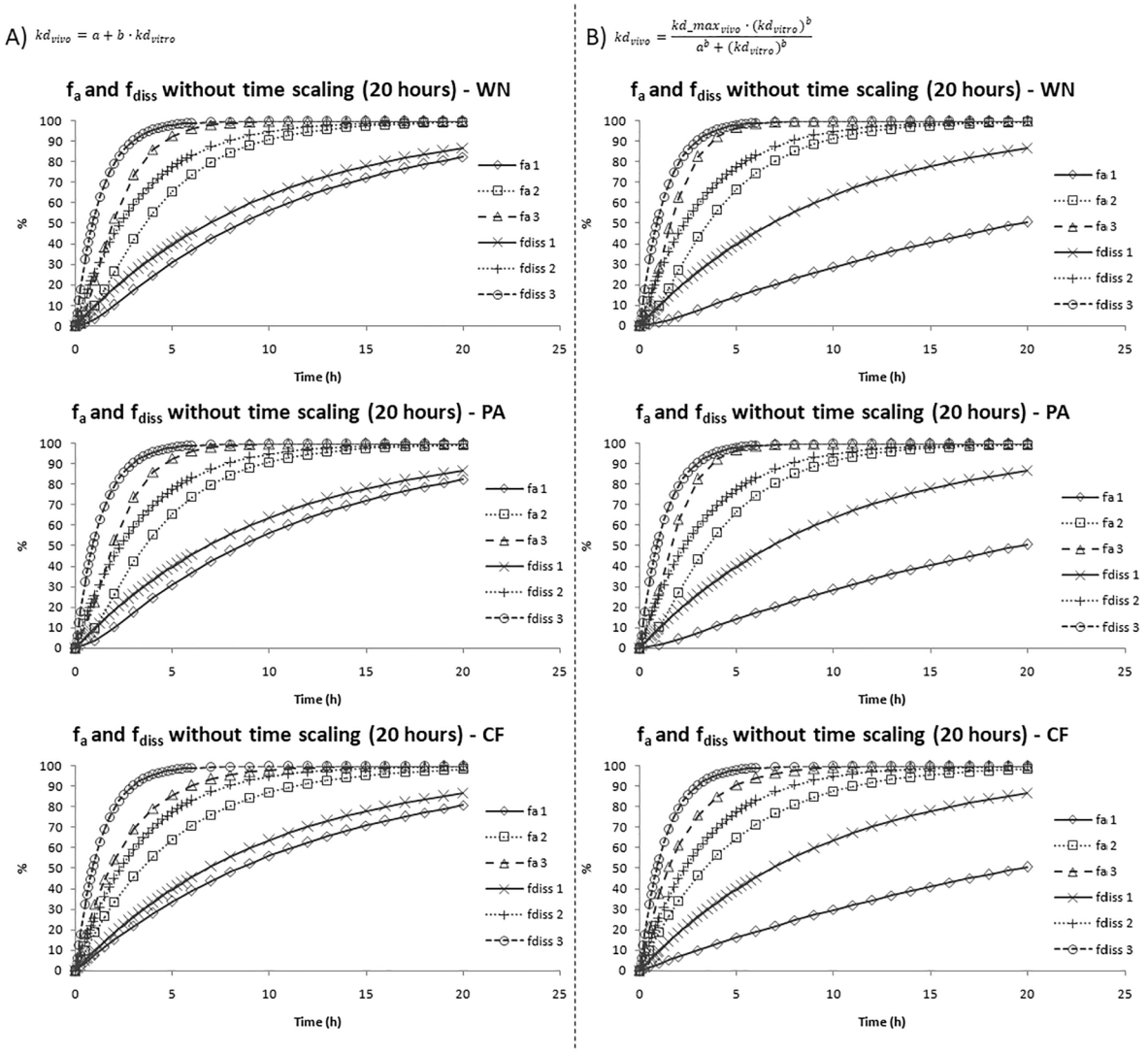

Fig. 3. Absorption and dissolution profiles represented in the real time scale. Profiles have been limited to 20 h to see more clearly if processes are or not superimposable. A) Absorption profiles from the *in vivo* data simulated assuming a linear relationship between the *in vitro* dissolution rate and the *in vivo* dissolution rate. B) Absorption profiles from the *in vivo* data simulated assuming a non-linear relationship between the *in vitro* dissolution rate and the *in vivo* dissolution rate.

which fractions dissolved were rescaled (Fig. 5). Fig. 5 shows fractions absorbed and fractions dissolved in the same graph after time scaling for those cases in which the Levy Plot was accepted.

$$\mathrm{IRF(Linear + Wagner - Nelson)} \rightarrow t_{vitro} = 0.898 \cdot t_{vivo} - 0.791 \quad (9)$$

$$\mathrm{IRF(Linear + Point - area)} \rightarrow t_{vitro} = 0.890 \cdot t_{vivo} - 0847 \quad (10)$$

$$\mathrm{IRF(Linear + Curve\ \ fitting)} \rightarrow t_{vitro} = 0.661 \cdot t_{vivo} + 0.080 \quad (11)$$

$$\mathrm{IRF(Non - linear + Curve\ \ fitting)} \rightarrow t_{vitro} = 0.498 \cdot t_{vivo} + 0.649 \quad (12)$$

3.4. Two-step in vitro-in vivo correlations

In total, 9 different IVIVCs were obtained for the simulated data in which *in vivo* dissolution rates has a linear relationship with the *in vitro* dissolution rates by relating f_{diss} and f_a at the same times. Table 1 summarizes the characteristics of all these correlations.

Firstly, it was tried to obtain linear level A IVIVCs without scaling the *in vitro* dissolution profiles, as the difference between absorption and dissolution did not seem very big (Fig. 3A), these correlations are shown in Fig. 6A. Also, they were obtained three linear correlations relating absorption and dissolution profiles after time scaling (Fig. 6B) and, additionally, to see if increasing the complexity of the correlation can prevent Levy plot from being done, three polynomial IVIVCs without time scaling were developed, they are shown in Fig. 6C.

For the simulated data in which a non-linear relationship between *in vivo* dissolution rates and *in vitro* dissolution rates was assumed, only a linear IVIVC after time scaling was obtained by relating f_{diss} and f_a from the curve fitting deconvolution method at the same times (Fig. 7), as the rest of levy plot were not good enough (Fig. 4) and without time scaling *in vitro* and *in vivo* profiles were not overlapping (Fig. 3B).

3.5. Convolution and internal validation

As it can be seen in Table 1, all the correlations for the simulated data in which *in vivo* dissolution rates have a linear relationship with the *in vitro* dissolution rates have a coefficient of determination (r^2) equal or higher than 0.970. Nevertheless, for deciding which correlation is the best one, internal validation must be done, and for it, predicted fractions absorbed must be convoluted to predicted plasma profiles. Fig. 8 shows the results of the convolution by the back Wagner-Nelson and the superposition methodology for the linear IVIVCs without time scaling and in Figs. 9 and 10 the same is shown for the linear IVIVCs with time scaling and the polynomial IVIVCs without time scaling, respectively.

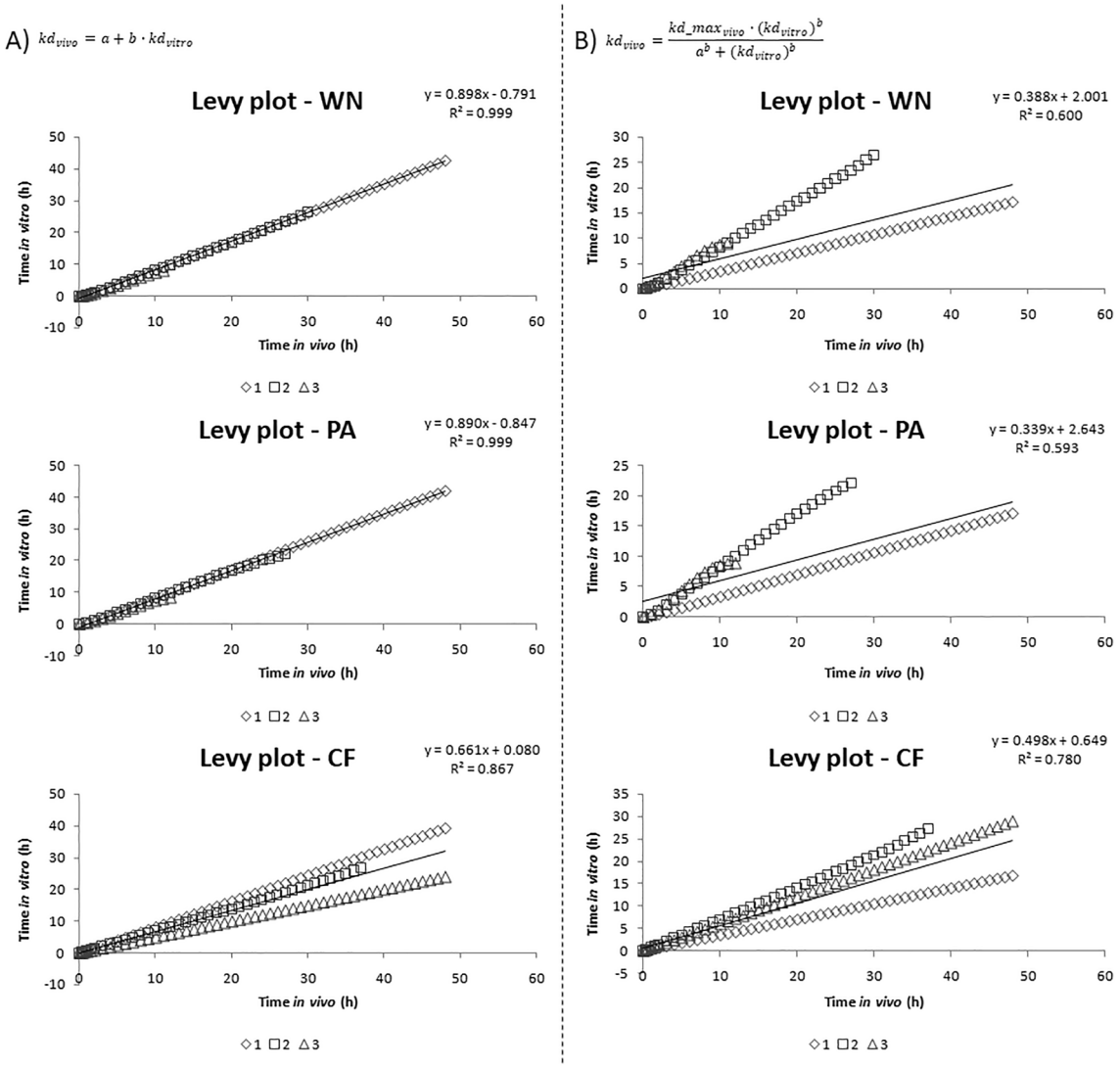

Fig. 4. Levy plots for each deconvolution approach. WN: Wagner-Nelson, PA: Point-area and CF: Curve fitting. A) Linear relationship between the *in vitro* dissolution rate and the *in vivo* dissolution rate. B) Non-linear relationship between the *in vitro* dissolution rate and the *in vivo* dissolution rate.

The prediction error percentages for all these IVIVCs, formulations and convolution methods are shown in Table 2. From them, it can be concluded that all the linear correlations with time scaling and all the polynomial correlations without time scaling are valid and bio-predictive, as, in all that cases, the mean prediction error for each parameter is lower than 10% and the prediction error for each formulation and each parameter is below 15%, but the linear IVIVCs without time scaling are not valid.

On the other hand, Table 3 shows the prediction error percentages for the two-step IVIVC obtained for the simulated data in which a non-linear relationship between *in vivo* dissolution rates and *in vitro* dissolution rates was assumed (Fig. 7). This IVIVC is not valid for both convolution methods, the back Wagner-Nelson and the superposition methodology, so with this type of data the two-step approach is not appropriate and the one-step one should be tested.

3.6. One-step in vitro-in vivo correlations

The supplementary material S1 shows the libraries that were used with the software Berkeley-Madonna for obtaining the one-step IVIVC for both types of simulated data, the ones in which the *in vivo* dissolution rates have a linear relationship with the *in vitro* dissolution rate and, the ones in which it is assumed that this relationship is non-linear. The model is general and it is summarized in equations (13)–(16), the only difference between one and other is the initial estimates for m and n, the slope and the intercept of the equation that relates the *in vivo* dissolution rate and the *in vitro* dissolution rate.

$$\frac{df_{diss}}{dt} = F_{max}22C5k_d \cdot e^{-k_d \cdot t} \tag{13}$$

$$\frac{dQ_{diss}}{dt} = \left(D.\frac{F_{max}}{100}.k_{d\_sc} \cdot e^{-k_{d\_sc} \cdot t} \cdot sc\right) - k_a \cdot Q_{diss\_vivo} \tag{14}$$

$$\frac{dQ_c}{dt} = k_a \cdot Q_{diss\_vivo} - k_{el} \cdot Q_c \tag{15}$$

$$C_p = \frac{Q_c}{V_d} \tag{16}$$

Equation (13) represents the *in vitro* dissolution process which was adjusted to a first order model, equation (14) represents the *in vivo* variation of amount of drug dissolved during time, which was obtained after scaling the *in vitro* dissolution rate (Eq. (17)) and adding a scale factor (sc), and equation (15) represents the amount of drug in the organism (central compartment) that if is divided by the distribution volume (V_d) gives the plasma concentrations (Cp) (Eq. (16)). Table 4

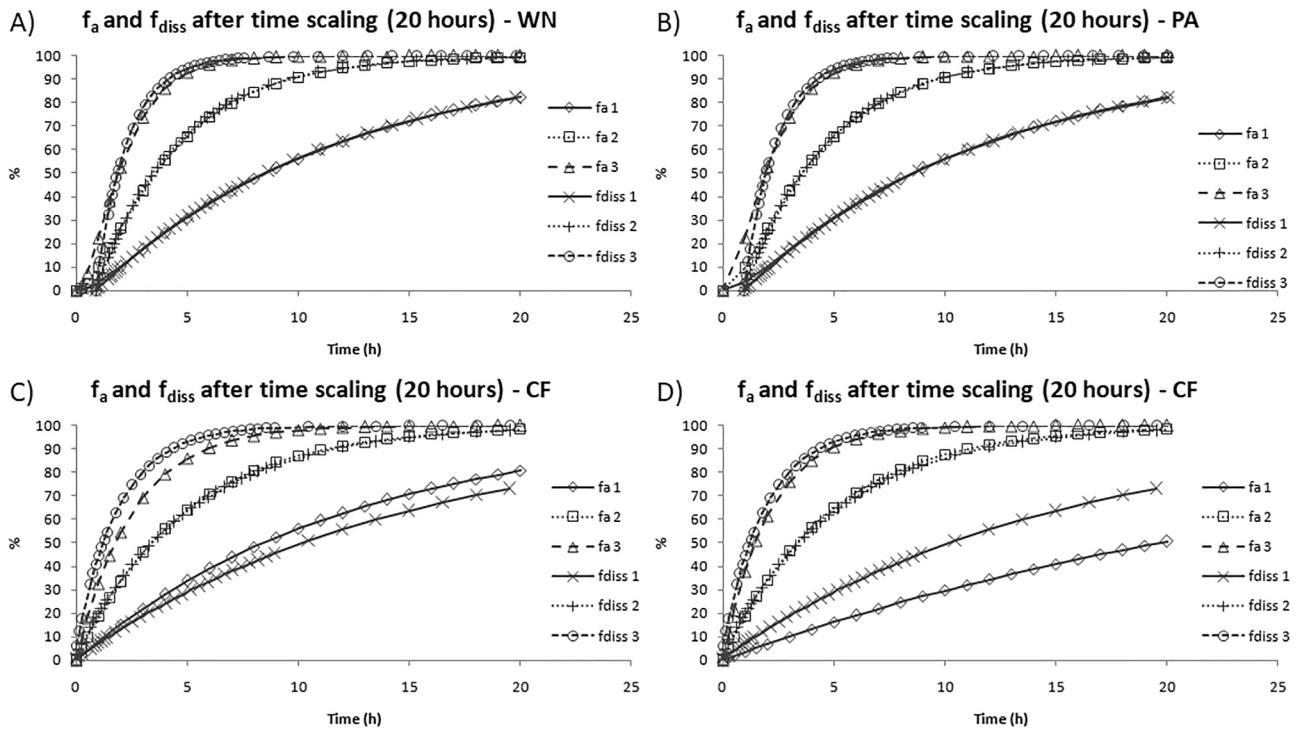

Fig. 5. Absorption and dissolution profiles represented after time scaling. Profiles has been limited to 20 h to see more clearly if processes are or not superimposable. A) linear f_a by Wagner-Nelson, B) linear f_a by point-area, C) linear f_a by curve fitting and D) non-linear f_a by curve fitting.

Table 1
Characteristics of the two-step IVIVCs obtained for the simulated data assuming that *in vivo* dissolution rates have a linear relationship with the *in vitro* dissolution rates.

IVIVC	Characteristics	r^2
L - WN + NL	Linear IVIVC (Wagner-Nelson without time scaling)	0.972
L - PA + NL	Linear IVIVC (Point-area without time scaling)	0.971
L - CF + NL	Linear IVIVC (Curve fitting without time scaling)	0.973
L - WN + L	Linear IVIVC (Wagner-Nelson with time scaling)	0.995
L - PA + L	Linear IVIVC (Point-area with time scaling)	0.992
L - CF + L	Linear IVIVC (Curve fitting with time scaling)	0.985
P - WN + NL	Polynomial IVIVC (Wagner-Nelson without time scaling)	0.987
P - PA + NL	Polynomial IVIVC (Point-area without time scaling)	0.986
P - CF + NL	Polynomial IVIVC (Curve fitting without time scaling)	0.987

shows the initial and final estimates for all the parameters used in the models.

The scale between the *in vitro* dissolution rate (k_d) and the *in vivo* dissolution rate (k_{d_sc}) was established with the equation (17) in which m and n initial estimates were obtained from the relation between the *in vitro* dissolution rate and the apparent *in vivo* absorption rate (k_a) obtained during the development of the two-step IVIVCs.

$$k_{d\_sc} = m \cdot k_d + n \tag{17}$$

Fig. 11 shows the experimental plasma profiles and the predicted plasma profiles obtained with the one-step approach, in which convolution is not necessary, it can be seen that predictions for both type of simulated data are almost overlapping the experimental values. Furthermore, according to Table 5 both IVIVCs are valid and biopredictive, so the one-step approach is appropriate in both cases: a) when there is a linear relationship between the *in vitro* dissolution rate and the *in vivo* dissolution rate and b) when there is a non-linear relationship between the *in vitro* dissolution rate and the *in vivo* dissolution rate.

4. Discussion

As it can be seen in Fig. 1, in this study *in vitro* dissolution profiles and *in vivo* plasma profiles were simulated for three different non-bioequivalent formulations which is the ideal situation for the development of an *in vitro-in vivo* correlation as it means that a dissolution test able to distinguish between different types of formulations has been found. Additionally, having a high difference between the profiles of the formulations is also good, as if the IVIVC is obtained it will be able to be used for predicting the *in vivo* profiles of all the formulations with a dissolution rate between the faster and the slower formulations used for developing the IVIVC.

In some occasions, the relation between the *in vitro* dissolution rate and the *in vivo* dissolution rate is not linear [30]. This happens, for example, when *in vivo* dissolution is site-dependent, as it was observed by Kim *et al* when working with sildenafil formulations [31]. Because of that, in this work two different batches of *in vivo* data were simulated, one in which it was assumed that the *in vivo* dissolution rate had a linear relationship with the *in vitro* dissolution rate and, a second one in which it was assumed that this relationship was non-linear and it followed a Hill equation (Fig. 1).

Regarding the absorption profiles of both types of *in vivo* data, shown in Fig. 2, it seems that all the profiles of f_a versus time obtained by the three deconvolution methods are quite similar and the same happens with their overlap with the *in vitro* dissolution profiles (Fig. 3). So, all the deconvolution methods, Wagner-Nelson method, point-area method and curve fitting method, could be considered a good option for transforming plasma profiles into absorption profiles, regardless of whether the relationship between dissolution rates is linear or non-linear. However, at this point, any conclusion about which is the best deconvolution method can be extracted and, for having that information, the different correlations must be obtained, and their predictability must be compared.

If the graphs before and after time scaling are compared (Figs. 3 and 5) it can be seen that, for the simulated data in which there is a linear relationship between dissolution rates, although having quite similar

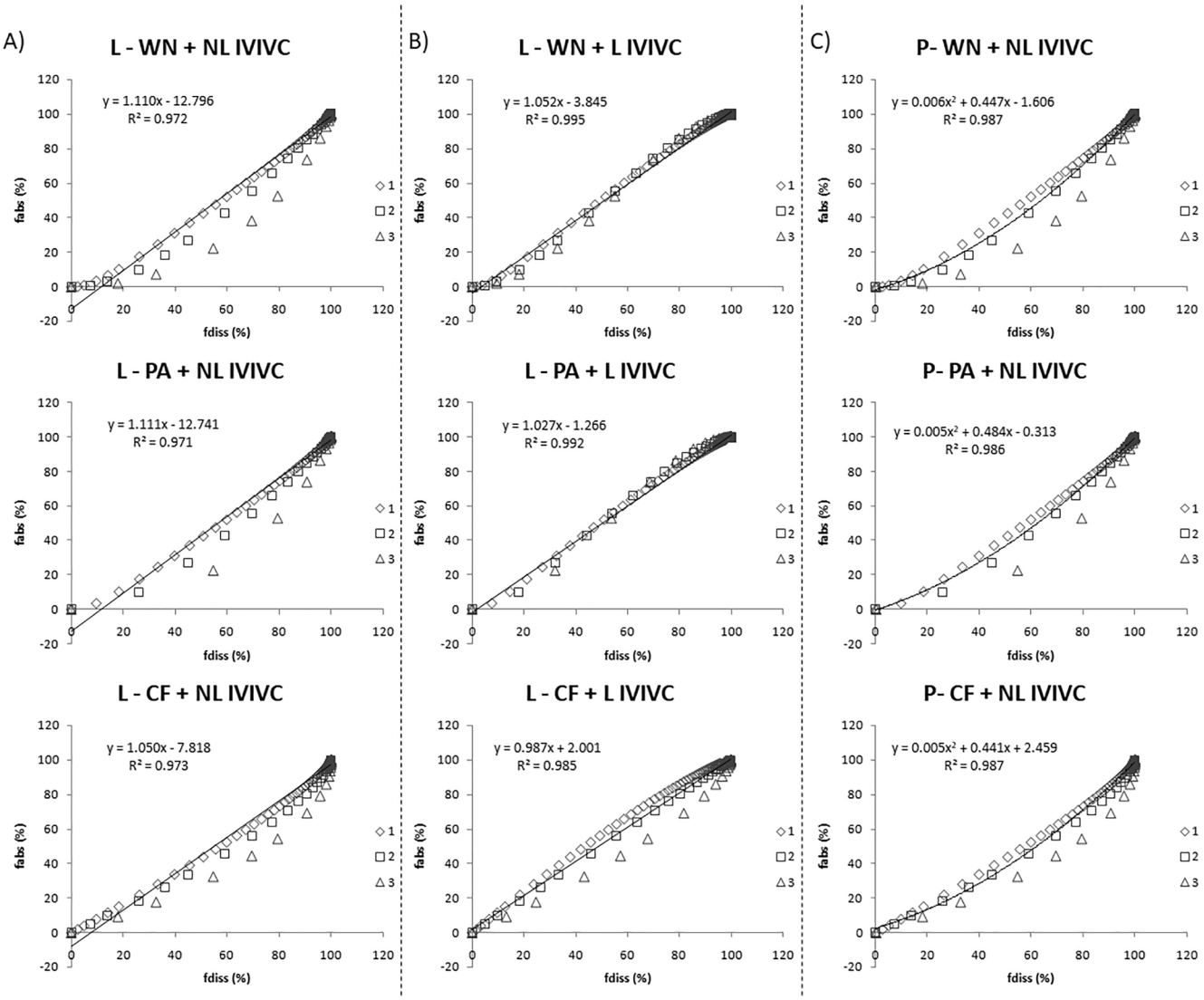

Fig. 6. Two-step IVIVCs obtained for the data simulated assuming a linear relationship between the *in vitro* dissolution rate and the *in vivo* dissolution rate. A) Linear IVIVCs without time scaling, B) Linear IVIVCs after time scaling and C) Polynomial IVIVCs without time scaling. WN: Wagner-Nelson, PA: Point-area and CF: Curve fitting.

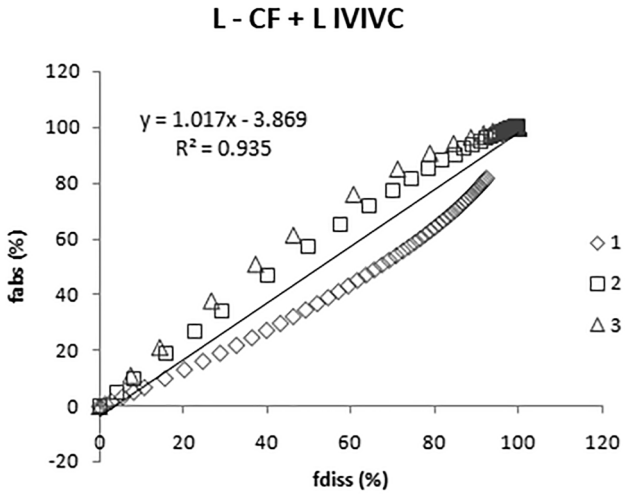

Fig. 7. Linear two-step IVIVC after time scaling obtained for the data simulated assuming a non-linear relationship between the *in vitro* dissolution rate and the *in vivo* dissolution rate. CF: Curve fitting.

dissolution and absorption profiles their overlap can be improved by the construction of a Levy plot and the obtaining of an inverse release function (Fig. 4) [20,25–27]. On the other hand, for the simulated data in which the relationship between dissolution rates is non-linear, it can be seen that the construction of a Levy plot is much more difficult (Fig. 4) as the slope of one of the formulations is completely different to the slope of the other two, especially, when Wagner-Nelson and point-area deconvolution methods are used. So the only absorption profiles that were time scaled from this data were those obtained by the curve fitting deconvolution method (Fig. 5).

Nevertheless, it must be taken into account that time scaling is not always necessary and, for discussing the necessity of having time scaling when using the two-step approach for obtaining a new IVIVC, in this study, three different types of *in vitro-in vivo* correlations were developed for the simulated data with a linear relationship between dissolution rates: linear IVIVC without time scaling, linear IVIVC after time scaling and polynomial IVIVC without time scaling (Fig. 6). All these correlations have a coefficient of determination (r^2) higher than 0.970 (Table 1). The correlations with the lowest r^2 are the linear ones obtained before time scaling, while the coefficient of determination increases whether a polynomial IVIVC is obtained without time scaling or

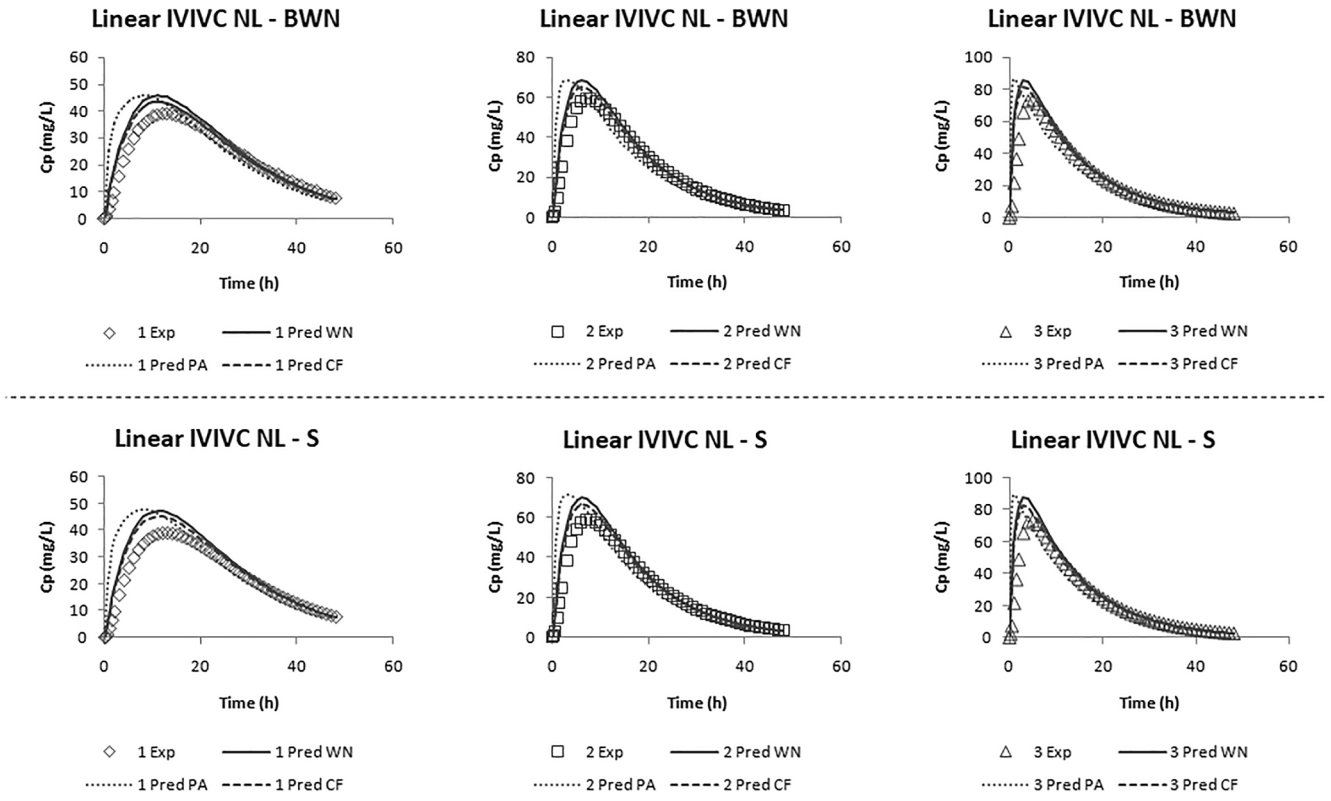

Fig. 8. Comparison of the experimental plasma profiles with the predicted ones by the back Wagner-Nelson (BWN) convolution method (top) and the superposition (S) methodology (bottom) for the linear two-step IVIVCs without time scaling obtained for the data simulated assuming a linear relationship between the *in vitro* dissolution rate and the *in vivo* dissolution rate. WN: Wagner-Nelson, PA: Point-area and CF: Curve fitting, NL: No Levy plot.

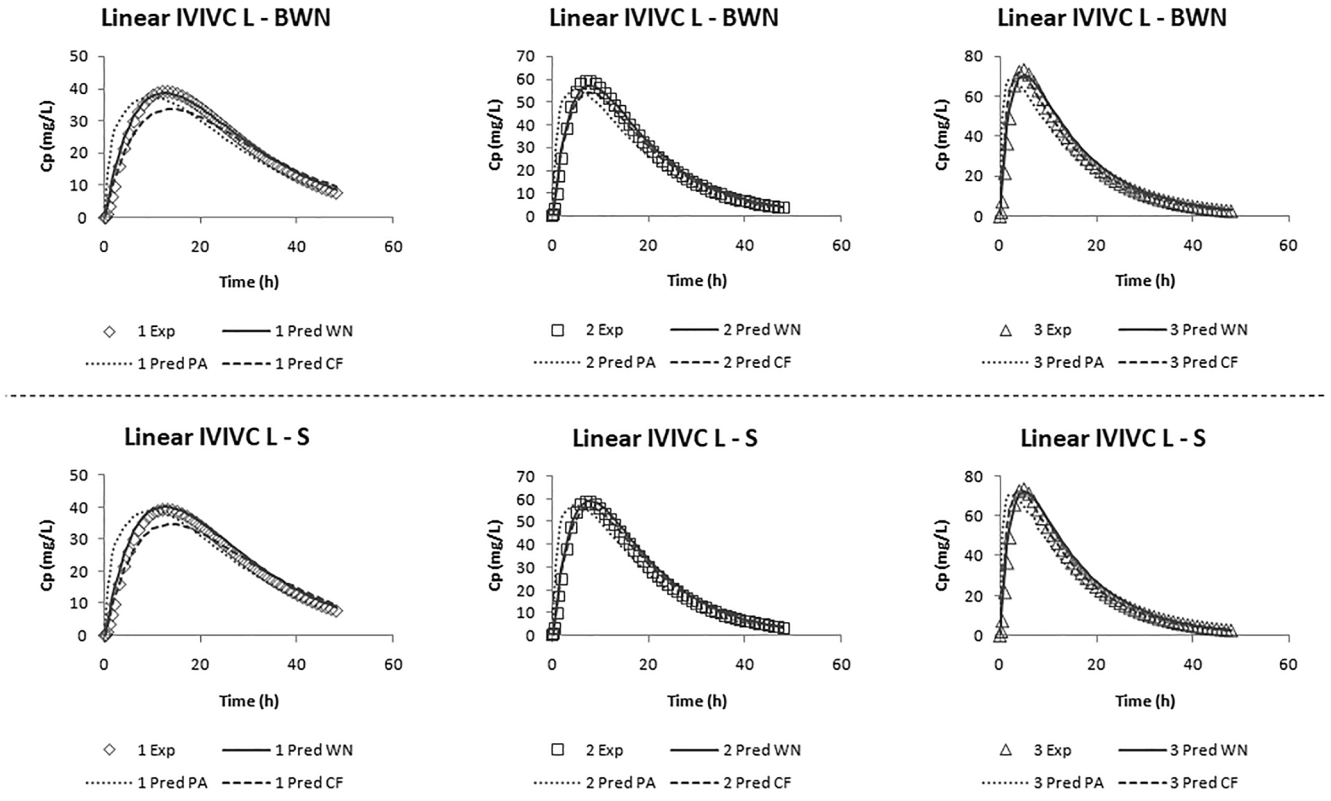

Fig. 9. Comparison of the experimental plasma profiles with the predicted ones by the back Wagner-Nelson (BWN) convolution method (top) and the superposition (S) methodology (bottom) for the linear two-step IVIVCs after time scaling obtained for the data simulated assuming a linear relationship between the *in vitro* dissolution rate and the *in vivo* dissolution rate. WN: Wagner-Nelson, PA: Point-area and CF: Curve fitting, L: Levy plot.

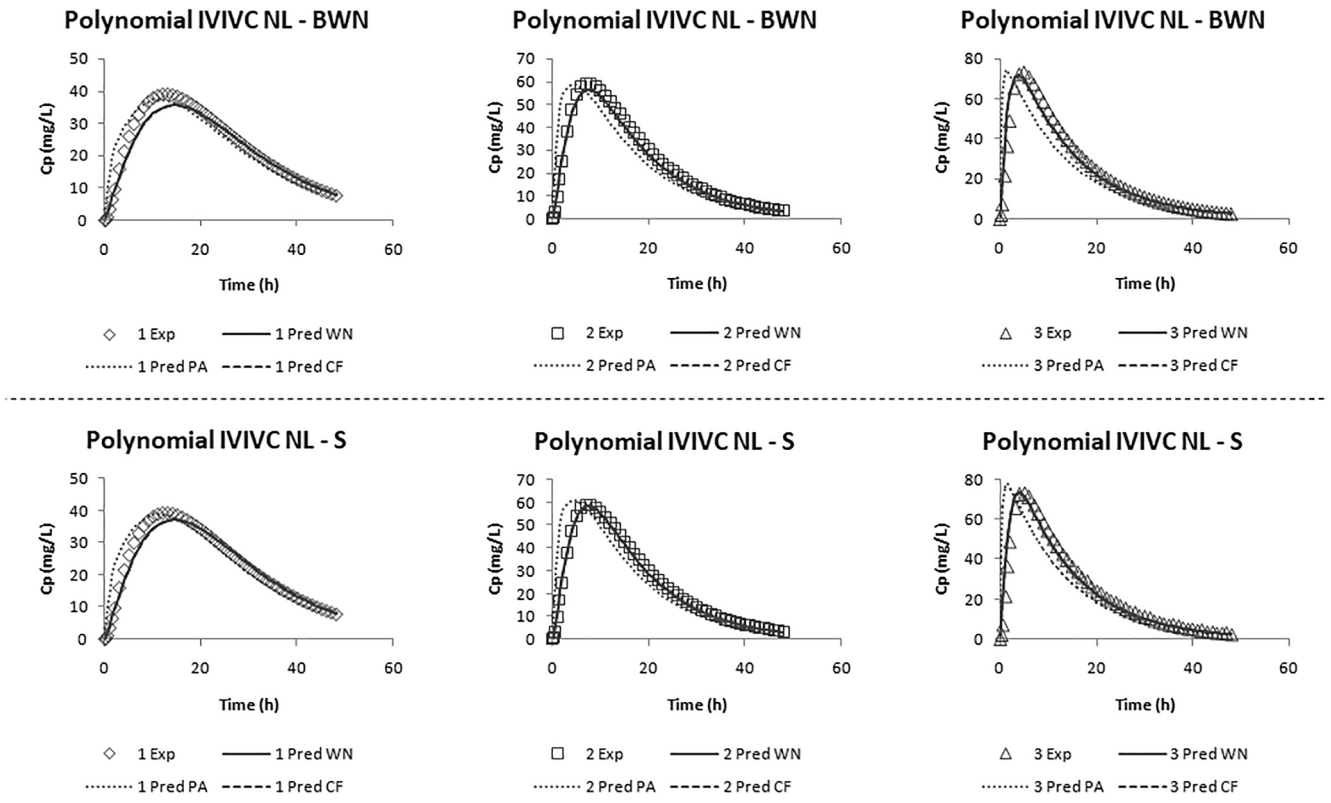

Fig. 10. Comparison of the experimental plasma profiles with the predicted ones by the back Wagner-Nelson (BWN) convolution method (top) and the superposition (S) methodology (bottom) for the polynomial two-step IVIVCs without time scaling obtained for the data simulated assuming a linear relationship between the *in vitro* dissolution rate and the *in vivo* dissolution rate. WN: Wagner-Nelson, PA: Point-area and CF: Curve fitting, NL: No Levy plot.

Table 2
Prediction errors of Cmax and AUC values forall the IVIVCs obtained for the simulated data assuming that *in vivo* dissolution rates have a linear relationship with the *in vitro* dissolution rates.

Linear IVIVCs without time scaling												
	Back Wagner-Nelson						Superposition method					
	Wagner-Nelson		Point-area		Curve fitting		Wagner-Nelson		Point-area		Curve fitting	
	AUC 0→∞	Cmax	AUC 0→∞	Cmax	AUC 0→∞	Cmax	AUC 0→∞	Cmax	AUC 0→∞	Cmax	AUC 0→∞	Cmax
1	11.72	17.17	11.80	17.31	6.88	11.45	15.78	21.35	16.33	22.03	10.71	15.38
2	11.08	16.28	11.10	16.51	6.32	10.38	14.43	19.65	15.61	21.18	9.49	13.55
3	11.16	17.14	11.13	17.73	6.40	11.03	13.53	19.42	15.63	22.45	8.65	13.16
Total	11.32	16.86	11.34	17.18	6.53	10.95	14.58	20.14	15.86	21.89	9.61	14.03
	NO VALID		**NO VALID**		**NO VALID**		**NO VALID**		**NO VALID**		**NO VALID**	

Linear IVIVCs with time scaling												
	Back Wagner-Nelson						Superposition method					
	Wagner-Nelson		Point-area		Curve fitting		Wagner-Nelson		Point-area		Curve fitting	
	AUC 0→∞	Cmax	AUC 0→∞	Cmax	AUC 0→∞	Cmax	AUC 0→∞	Cmax	AUC 0→∞	Cmax	AUC 0→∞	Cmax
1	4.46	0.70	1.78	3.90	2.82	13.96	8.33	2.93	5.90	0.03	0.78	10.80
2	5.25	3.32	2.66	6.44	0.18	8.27	8.73	0.20	6.82	2.68	3.05	5.35
3	5.32	3.73	2.68	6.79	0.17	2.02	8.23	1.19	7.01	3.05	2.24	0.21
Total	5.01	2.58	2.38	5.71	1.06	8.09	8.43	1.44	6.58	1.92	2.02	5.45
	VALID		**VALID**		**VALID**		**VALID**		**VALID**		**VALID**	

Polynomial IVIVCs without time scaling												
	Back Wagner-Nelson						Superposition method					
	Wagner-Nelson		Point-area		Curve fitting		Wagner-Nelson		Point-area		Curve fitting	
	AUC 0→∞	Cmax	AUC 0→∞	Cmax	AUC 0→∞	Cmax	AUC 0→∞	Cmax	AUC 0→∞	Cmax	AUC 0→∞	Cmax
1	5.08	8.36	1.49	4.67	4.63	8.42	1.46	4.87	2.50	0.84	1.04	4.97
2	5.23	4.43	1.71	0.69	4.73	4.70	2.07	1.30	2.27	3.30	1.59	1.62
3	5.16	1.56	1.68	2.32	4.65	1.94	2.86	0.76	2.30	6.43	2.37	0.33
Total	5.16	4.78	1.63	2.56	4.67	5.02	2.13	2.31	2.35	3.52	1.66	2.31
	VALID		**VALID**		**VALID**		**VALID**		**VALID**		**VALID**	

Table 3
Prediction errors of Cmax and AUC values for the IVIVC obtained for the simulated data assuming that *in vivo* dissolution rates have a non-linear relationship with the *in vitro* dissolution rates.

Linear IVIVCs with time scaling				
	Back Wagner-Nelson		Superposition method	
	Curve fitting		Curve fitting	
	AUC 0→∞	Cmax	AUC 0→∞	Cmax
1	15.22	31.26	19.53	36.15
2	2.92	11.90	6.36	9.04
3	3.03	16.78	6.06	14.41
Total	7.06	19.98	10.65	19.87
	NO VALID		NO VALID	

Table 4
Initial and final estimates for the parameters of the model used for obtaining one-step IVIVCs.

	Linear simulated data		Non-linear simulated data	
Parameter	Initial	Final	Initial	Final
k_{d1} (h^{-1})	0.10138	0.10138	0.10138	0.10138
F_{max1} (%)	99.975	99.975	99.975	99.975
k_{d2} (h^{-1})	0.29787	0.29787	0.29787	0.29787
F_{max2} (%)	99.986	99.986	99.986	99.986
k_{d3} (h^{-1})	0.79036	0.79036	0.79036	0.79036
F_{max3} (%)	100	100	100	100
Dose (mg)	100	100	100	100
k_{el} (h)	0.08	0.08	0.08	0.08
V_d(L)	1	1	1	1
m	0.736	0.897325*	1.007	1.20588*
n (h^{-1})	0.024	0.00027*	−0.057	−0.085*
k_a (h^{-1})	1	1.12959*	1	1.18*
sc	1	0.999935*	1	0.999897*

* indicates that the initial and the final estimates are different

a linear correlation is developed after time scaling. This is what might be expected, as increasing the complexity of a mathematical model, increases by force its r^2 [32]. So for evaluating the goodness of a correlation the value of the coefficient of determination cannot be the only thing to look, an internal validation is needed.

In the case of the simulated data with a non-linear relationship between dissolution rates only a linear IVIVC after time scaling was obtained after the deconvolution by the curve fitting method (Fig. 7), this correlation has a r^2 of 0.935, but, as in the other case, an internal validation is needed to evaluate its predictability.

As two-step IVIVCs relate dissolved fractions with absorbed fractions, for internal validation, predicted absorbed fractions must be convoluted to plasma profiles. Figs. 8, 9 and 10 show the comparison of the experimental and the predicted plasma profiles after convolution by back Wagner-Nelson method and superposition method for all the IVIVCs obtained for the simulated data with a linear relationship between dissolution rates. In general, all the predictions are quite similar, although the worst profiles seem to be those obtained from the linear IVIVC without time scaling (Fig. 8). This fact is confirmed when prediction error percentages are calculated (Table 2) as for the linear IVIVCs without time scaling, they are higher than the pre-established limits and the correlations are not valid. In the case of the linear IVIVCs with time scaling and the polynomial IVIVCs without time scaling, they are valid and biopredictive as all the PE% are below the limits (the mean prediction error for each parameter is lower than 10% and the prediction error for each formulation and each parameter is below 15%).

From the above, it can be extracted that two different approaches can be used for obtaining a valid IVIVC when the direct linear IVIVC without time scaling is not valid. *In vitro* dissolution profiles can be scaled on terms of time or the complexity of the correlation can be increased by adding parameters without time scaling the dissolution profiles. Furthermore, it has been seen that, for the simulated data with a linear relationship between dissolution rates, valid and biopredictive correlations have been obtained using all the deconvolution and convolution methods and all of them have similar PE%, so, this means that any combination of methods could be used for obtaining a two-step IVIVC when the relationship between *in vitro* dissolution rate and the *in vivo*

Table 5
Prediction errors of Cmax and AUC values for the IVIVCs obtained using the one-step approach.

	Linear simulated data		Non-linear simulated data	
	AUC 0→∞	Cmax	AUC 0→∞	Cmax
1	0.00	0.02	0.16	0.07
2	0.02	0.02	0.01	0.05
3	2.67	0.01	2.57	1.51
Total	0.90	0.02	0.91	0.54
	VALID		**VALID**	

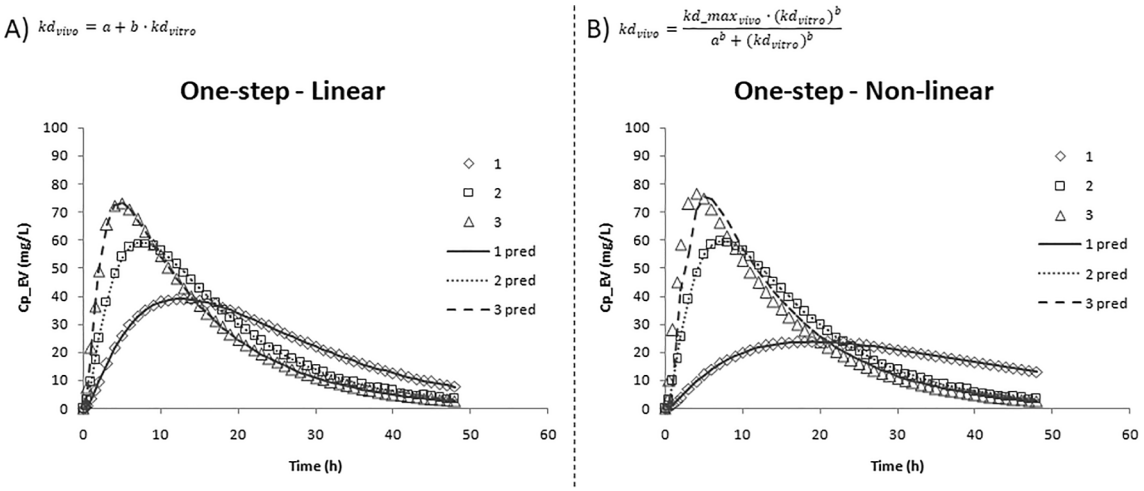

Fig. 11. Comparison of the experimental plasma profiles and the predicted ones by the one-step IVIVCs. A) Absorption profiles from the *in vivo* data simulated assuming a linear relationship between the *in vitro* dissolution rate and the *in vivo* dissolution rate. B) Absorption profiles from the *in vivo* data simulated assuming a non-linear relationship between the *in vitro* dissolution rate and the *in vivo* dissolution rate.

dissolution rate is linear. It has not been found the best combination of deconvolution-convolution methods, but for reaching this aim more studies with a wider range of one-compartment and dissolution profiles would be needed.

The two-step IVIVC obtained for the simulated data with a non-linear relationship between dissolution rates was not valid (Table 3) as its prediction errors were too high. Thus, the alternative for obtaining an IVIVC for this type of data is the one-step approach. Fig. 11 shows a comparison of the experimental and the predicted plasma profiles by the one-step IVIVCs for both types of simulated data. The developed model was biopredictive both when the relationship between dissolution rates is linear and when the relationship between rates is non-linear and its prediction errors were extremely low (Table 5). So, the modelling and the one-step approach can be considered a useful tool when an IVIVC is developed as it can overcome some problems that the two-step approach cannot.

5. Conclusion

Twelve valid and bio predictive two-step level A IVIVCs, whose percentages of prediction error are lower than the pre-established limits, have been developed for *in vitro* and *in vivo* simulated data with a linear relationship between their dissolution rates.

Results highlight the importance of time scaling to obtain valid and bio predictive correlations that can be used as substitutes of human bioequivalence studies; as, if it is not done, the complexity of the correlation must be increased.

There is not a combination of deconvolution and convolution methods that could be named as the best one, if in the valid two-step correlations all the prediction errors for any combination are within the limits.

It was not possible to obtain a valid and biopredictive two-step level A IVIVC when the *in vitro* and *in vivo* simulated data had a non-linear relationship between their dissolution rates, but the one-step approach was able to overcome this fact and it was able to give valid IVIVCs regardless of whether the relationship between dissolution rates is linear or non-linear.

To sum up, results agree to what is generally expected and described from these approaches but have the major relevance of identifying the probable reasons and possible solutions for increasing the chances of obtaining valid IVIVC. Regarding future expectations, it is important to note that in order to get strong conclusions work should continue on comparing deconvolution and convolution methods with other simulated data, but also with experimental data to see if always the same results are achieved.

Declaration of Competing Interest

The authors declare that they have no known competing financial interests or personal relationships that could have appeared to influence the work reported in this paper.

Acknowledgements

Funding: This work was supported by the Agencia Estatal Investigación and European Union, through FEDER (Fondo Europeo de Desarrollo Regional) [SAF2016-78756(AEI/FEDER, EU), "Modelos *in vitro* de evaluación biofarmaceutica"]. Bárbara Sánchez-Dengra received a grant from the Ministry of Science, Innovation and Universities of Spain [FPU17/00530].

Appendix A. Supplementary material

Supplementary data to this article can be found online at https://doi.org/10.1016/j.ejpb.2020.11.009.

References

[1] G.L. Amidon, H. Lennernäs, V.P. Shah, J.R. Crison, A theoretical basis for a biopharmaceutic drug classification: the correlation of in vitro drug product dissolution and in vivo bioavailability, Pharm. Res. An Off. J. Am. Assoc. Pharm. Sci. 12 (1995) 413–420, https://doi.org/10.1023/A:1016212804288.
[2] EMA - Committee for Medicinal Products for Human Use (CHMP), Guideline on the investigation of bioequivalence, 1997. http://www.ema.europa.eu (accessed January 16, 2020).
[3] FDA, Waiver of In Vivo Bioavailability and Bioequivalence Studies for Immediate-Release Solid Oral Dosage Forms Based on a Biopharmaceutics Classification System Guidance for Industry, 2017. http://www.fda.gov/Drugs/GuidanceComplianceRegulatoryInformation/Guidances/default.htm (accessed January 16, 2020).
[4] FDA, Guidance for Industry - Extended Release Oral Dosage Forms: Development, Evaluation, and Application of In Vitro/In Vivo Correlations, Tel, 1997. http://www.fda.gov/cder/guidance/index.htm (accessed January 16, 2020).
[5] EMA - Committee for Medicinal Products for Human Use (CHMP), Guideline on the pharmacokinetic and clinical evaluation of modified release dosage forms (EMA/CPMP/EWP/280/96 Corr1), 2014. http://www.ema.europa.eu/contact (accessed January 16, 2020).
[6] A. Chowdhury, S. Islam, In vitro–in vivo correlation as a surrogate for bioequivalence testing: the current state of play, Asian J. Pharm. Sci. 6 (2011) 176–190 (accessed September 1, 2020), http://asianjps.syphu.edu.cn/EN/article/downloadArticleFile.do?attachType=PDF&id=177.
[7] J. Emami, In vitro - in vivo correlation: from theory to applications, J. Pharm. Pharm. Sci. 9 (2006) 169–189 (accessed September 1, 2020), https://pubmed.ncbi.nlm.nih.gov/16959187/.
[8] J.A. Cook, Development strategies for IVIVC in an industrial environment, Biopharm. Drug Dispos. 33 (2012) 349–353, https://doi.org/10.1002/bdd.1791.
[9] C. Costello, S. Rossenu, A. Vermeulen, A. Cleton, A. Dunne, A time scaling approach to develop an in vitro-in vivo correlation (IVIVC) model using a convolution-based technique, J. Pharmacokinet. Pharmacodyn. 38 (2011) 519–539, https://doi.org/10.1007/s10928-011-9206-4.
[10] E. Soto, S. Haertter, M. Koenen-Bergmann, A. Staab, I.F. Trocóniz, Population in vitro-in vivo correlation model for pramipexole slow-release oral formulations, Pharm. Res. 27 (2010) 340–349, https://doi.org/10.1007/s11095-009-0027-8.
[11] EMA, Guideline on quality of oral modified release products, 2014. http://www.ema.europa.eu (accessed September 1, 2020).
[12] C. Csajka, D. Drover, D. Verotta, The use of a sum of inverse gaussian functions to describe the absorption profile of drugs exhibiting complex absorption, Pharm. Res. 22 (2005) 1227–1235, https://doi.org/10.1007/s11095-005-5266-8.
[13] D.R. Drover, M.S. Angst, M. Valle, B. Ramaswamy, S. Naidu, D.R. Stanski, D. Verotta, Input characteristics and bioavailability after administration of immediate and a new extended-release formulation of hydromorphone in healthy volunteers, Anesthesiology. 97 (2002) 827–863 (accessed September 1, 2020), http://www.anesthesiology.org.
[14] M. Pitsiu, G. Sathyan, S. Gupta, D. Verotta, A Semiparametric Deconvolution Model to Establish In Vivo–In Vitro Correlation Applied to OROS Oxybutynin, J. Pharm. Sci. 90 (2001) 702–712, https://doi.org/10.1002/jps.1026.
[15] A. Dunne, T. O'Hara, J. Devane, A new approach to modelling the relationship between in vitro and in vivo drug dissolution/absorption, Stat. Med. 18 (1999) 1865–1876, https://doi.org/10.1002/(SICI)1097-0258(19990730)18:14<1865::AID-SIM223>3.0.CO;2-P.
[16] G. Balan, P. Timmins, D.S. Greene, P.H. Marathe, In vitro-In vivo correlation (IVIVC) models for metformin after administration of modified-release (MR) oral dosage forms to healthy human volunteers, J. Pharm. Sci. 90 (2001) 1176–1185, https://doi.org/10.1002/jps.1071.
[17] S. Dutta, Y. Qiu, E. Samara, G. Cao, G.R. Granneman, Once-a-day extended-release dosage form of divalproex sodium III: Development and validation of a level A in vitro-in vivo correlation (IVIVC), J. Pharm. Sci. 94 (2005) 1949–1956, https://doi.org/10.1002/jps.20387.
[18] P. Veng-Pedersen, J.V.S. Gobburu, M.C. Meyer, A.B. Straughn, Carbamazepine level-A in vivo-in vitro correlation (IVIVC): A scaled convolution based predictive approach, Biopharm. Drug Dispos. 21 (2000) 1–6, https://doi.org/10.1002/1099-081X(200001)21:1<1::AID-BDD207>3.0.CO;2-D.
[19] M. Bermejo, J. Meulman, M.G. Davanço, P. de O. Carvalho, I. Gonzalez-Alvarez, D. R. Campos, In vivo predictive dissolution (Ipd) for carbamazepine formulations: Additional evidence regarding a biopredictive dissolution medium, Pharmaceutics 12 (2020) 1–21, https://doi.org/10.3390/pharmaceutics12060558.
[20] A. Figueroa-Campos, B. Sánchez-Dengra, V. Merino, A. Dahan, I. González-Álvarez, A. García-Arieta, M. González-Álvarez, M. Bermejo, Candesartan Cilexetil in vitro-in vivo correlation: predictive dissolution as a development tool, Pharmaceutics 12 (2020) 633, https://doi.org/10.3390/pharmaceutics12070633.
[21] M. Bermejo, G. Kuminek, J. Al-Gousous, A. Ruiz-Picazo, Y. Tsume, A. Garcia-Arieta, I. González-Alvarez, B. Hens, D. Mudie, G.E. Amidon, N. Rodriguez-Hornedo, G.L. Amidon, Exploring bioequivalence of dexketoprofen trometamol drug products with the gastrointestinal simulator (GIS) and precipitation pathways analyses, Pharmaceutics 11 (2019), https://doi.org/10.3390/pharmaceutics11030122.
[22] J. Domenech Berrozpe, I. Diez Martin, C. Peraire Guitart, Administración extravasal: aproximación compartimental, in: J. Domenech Berrozpe, J. Martinez Lanao, C. Peraire Guitart (Eds.), Tratado Gen. Biofarm. y Farm., vol. I, LADME., Síntesis, Madrid, 2015, pp. 297–366.
[23] I. González-García, V. Mangas-Sanjuán, M. Merino-Sanjuán, M. Bermejo, In vitro-in vivo correlations: General concepts, methodologies and regulatory applications,

Drug Dev. Ind. Pharm. 41 (2015) 1935–1947, https://doi.org/10.3109/03639045.2015.1054833.
[24] H. Cheng, W.J. Jusko, The area function method for assessing the drug absorption rate in linear systems with zero-order input, Pharm. Res. 6 (1989) 133–139, https://doi.org/10.1023/a:1015928509101.
[25] J.-M. Cardot, B.M. Davit, In vitro-in vivo correlations: tricks and traps, AAPS J. 14 (2012) 491–499, https://doi.org/10.1208/s12248-012-9359-0.
[26] A. Ruiz Picazo, M.T. Martinez-Martinez, S. Colón-Useche, R. Iriarte, B. Sánchez-Dengra, M. González-Álvarez, A. García-Arieta, I. González-Álvarez, M. Bermejo, In Vitro dissolution as a tool for formulation selection: Telmisartan two-step IVIVC, Mol. Pharm. 15 (2018) 2307–2315, https://doi.org/10.1021/acs.molpharmaceut.8b00153.
[27] J.M. Cardot, J.C. Lukas, P. Muniz, Time scaling for in vitro-in vivo correlation: the inverse release function (IRF) approach, AAPS J. 20 (2018) 95, https://doi.org/10.1208/s12248-018-0250-5.
[28] M.C. Gohel, R.R. Delvadia, D.C. Parikh, M. Zinzuwadia, C.D. Soni, N.R. Mehta, B. Joshi, A.S. Dabhi, Simplified Mathematical Approach for Back Calculation in Wagner - Nelson Method : Applications in In Vitro and In Vivo Correlation (IVIVC) and Formulation Development Work, (2005).
[29] F. Langenbucher, Handling of computational in vitro/in vivo correlation problems by Microsoft Excel: III. Convolution and deconvolution, Eur. J. Pharm. Biopharm. 56 (2003) 429–437, https://doi.org/10.1016/s0939-6411(03)00140-1.
[30] Y. Lu, S. Kim, K. Park, In vitro-in vivo correlation: Perspectives on model development, Int. J. Pharm. 418 (2011) 142–148, https://doi.org/10.1016/j.ijpharm.2011.01.010.
[31] T.H. Kim, S. Shin, S.W. Jeong, J.B. Lee, B.S. Shin, Physiologically relevant in vitro-in vivo correlation (IVIVC) approach for sildenafil with site-dependent dissolution, Pharmaceutics 11 (2019) 251, https://doi.org/10.3390/pharmaceutics11060251.
[32] B. Hu, J. Shao, Generalized linear model selection using R2, J. Stat. Plan. Inference. 138 (2008) 3705–3712, https://doi.org/10.1016/j.jspi.2007.12.009.